Published in Geochimica et Cosmochimica Acta 68/5 : 1021-1033, 2004,
which should be used for any reference to this work

Carbonate and silicate weathering in two presently glaciated, crystalline catchments in the Swiss Alps

R. HOSEIN, K. ARN, P. STEINMANN, T. ADATTE, and K. B. FÖLLMI*
Insititut de Géologie, Université de Neuchâtel, Rue Emile Argand 11, CH-2007, Neuchâtel, Switzerland

Abstract—We present a weathering mass balance of the presently glaciated Rhône and Oberaar catchments, located within the crystalline Aar massif (central Switzerland). Annual chemical and physical weathering fluxes are calculated from the monthly weighted means of meltwater samples taken from July, 1999 to May, 2001 and are corrected for precipitation inputs. The meltwater composition issuing from the Oberaar and Rhône catchments is dominated by calcium, which represents 81% and 55% of the total cation flux respectively (i.e. 555 and 82–96 keq km^{-2} yr^{-1}). The six to seven times higher Ca^{2+} denudation flux from the Oberaar catchment is attributed to the presence of a strongly foliated gneissic zone. The gneissic zone has an elevated calcite content (as reflected by the 4.6 times higher calcite content of the suspended sediments from Oberaar compared to Rhône) and a higher mechanical erosion rate (resulting in a higher flux of suspended sediment). The mean flux of suspended calcite of the Oberaar meltwaters during the ablation period is 7 times greater than that of the Rhône meltwaters. Taking the suspended calcite as a proxy for the total (including sub-glacial sediments) weathering calcite surface area, it appears that the available surface area is an important factor in controlling weathering rates. However, we also observe an increased supply of protons for carbonate dissolution in the Oberaar catchment, where the sulphate denudation flux is six times greater. Carbonic acid is the second important source of protons, and we calculate that three times as much atmospheric CO_2 is drawn down (short term) in the Oberaar catchment. Silica fluxes from the two catchments are comparable with each other, but are 100 kmol km^2 yr^{-1} lower than fluxes from physically comparable, non-glaciated basins.

1. INTRODUCTION

Glaciers and periods of glaciation may have a significant impact on global weathering, changing the interplay between physical and chemical weathering processes, by putting large volumes of dilute meltwaters and fine-grained sediment in contact with each other. Glaciers are significant agents of physical erosion; for example, the mechanical denudation of glaciated valleys in Alaska and Norway is an order of magnitude greater than that in equivalent non-glaciated basins (Hallet al., 1996). Hay (1998) suggests that today's global, glacially derived yield of detrital sediments is about half the fluvial detrital yield, but that the two systems' yields were possibly equal before the advent of man. Furthermore, the nature of glacially derived sediments may predispose them to higher rates of chemical weathering compared to sediments derived from fluvial erosion processes. Abrasion at the glacier sole generate large volumes of silt-sized grains (Dreimanis & Vagners, 1969, 1971; Boulton, 1979; Drewry, 1986) which are heavily indented and fractured (Mahaney, 1995 and references therein) leading to greater surface areas relative to volume, complicated micro-topographies and so increased chemical reactivities (White and Brantley, 1995 and references therein). Reaction of this sediment with dilute, close to neutral meltwaters leads to solute fluxes from glacial catchments that are three times the Summerfield (1991) estimated global average denudation rate of 14.8 t km^{-2} yr^{-1} (Sharp et al., 1995); this is strongly influenced by the large runoff volumes draining glacier-covered basins (Bluth and Kump, 1994). The characteristic chemical signature of glacial meltwaters is strongly linked to the susceptibility of minerals to comminution and the temperature dependence of mineral dissolution rates (White et al., 1999a). Catchment studies by numerous authors (e.g., Eyles et al., 1982; Drever and Hurcomb, 1986; Sharp et al., 1995; Anderson et al., 1997, 2000) find glacial meltwaters elevated in dissolved Ca^{2+} and K^+ relative to non-glacial runoff, but depressed with respect to silica (e.g., Anderson et al., 1997, 2000; West et al., 2002) due to the temperature dependent nature of silicate weathering (White et al., 1999a). It is widely concluded that the predominant reactions in glacial meltwaters are calcite dissolution and the non-stoichimetric hydrolysis of K^+ from micas (e.g., Drever and Hurcomb, 1986).

Calcite is milled into ultra-fine particles in the subglacial environment (Fairchild et al., 1999) increasing its chemical reactivity, and at near neutral pH the dissolution rate of calcite (10^{-5} mol m^{-2} s^{-1}; Plummer et al., 1978) is approximately 11 orders of magnitude faster than the dissolution rate of albite ($\approx$ 10^{-16} mol m^{-2} s^{-1}; Chou and Wollast, 1985). Calcite is not confined to catchments with carbonate geology; for example, is also present as an accessory mineral in crystalline rocks and as a secondary mineral in hydrothermal veins in areas that have undergone internal deformation (such as the Aar massif in our study). Therefore calcite may exert a strong influence on meltwater chemistry in such crystalline regions: White et al. (1999b) observed that calcite provides up to 98% of the calcium flux from freshly ground granitoid rocks in laboratory leaching experiments. Glacial weathering processes may optimise the dissolution of carbonates within catchments in crystalline areas: firstly as calcite and quartz are abraded more

* Author to whom correspondence should be addressed (karl.foellmi@unine.ch).

effectively when ground together rather than separately (Fairchild et al., 1999) and secondly because crystalline bedrock generally has a lower permeability than carbonate bedrock. Water pressures at the base of the Laurentide ice mass may have been greater in crystalline areas, facilitating basal slip and locally increasing erosion compared to areas of ice underlain by carbonate formations (Sugden, 1978). Crystalline rocks form over 20% of the continental area (granites = 10.4%, gneisses = 10.4%; Meybeck, 1987) and predominate over carbonate rocks at latitudes that were ice-covered at the Last Glacial Maximum (Gibbs and Kump, 1994 and references therein). Therefore, defining the relative contribution of calcite to weathering fluxes in presently glacier-covered, mono-lithological crystalline catchments is an important goal in assessing the potential feedbacks between glaciation, weathering of continental rocks and atmospheric CO_2 (e.g., Berner, 1991; Ludwig et al., 1998).

In this study we measure the influence of calcite on meltwater chemistries draining two small, presently glaciated, crystalline catchments in Switzerland, containing the Rhône and Oberaar glaciers. These geographically and glaciologically comparable watersheds are seated in the Aar massif, comprised of Hercynian aged granites and granodiorites, which contain detectable amounts of calcite (<1% interstitial calcite; Keusen et al., 1989). We assess the weathering intensity in these catchments by measuring the concentration of dissolved ions and suspended sediments in the meltwaters. Here we present the annual variation in meltwater composition of these catchments from 1999 to 2001, including samples taken during the two accumulation periods, when discharge is minimal and therefore sediment-water interaction times are of longer duration.

We observe that the silica fluxes from the two catchments are comparable with each other. In contrast the total cation flux from the Rhône glacier (147–175 keq km^{-2} yr^{-1}) is significantly below Livingstone's global average (390 keq km^{-2} yr^{-1}; Livingstone, 1963), whereas the Oberaar's total cation flux (681 keq km^{-2} yr^{-1}) is significantly higher (fluxes are corrected for precipitation inputs). Since the specific runoff from the Oberaar basin (2.4 m yr^{-1}) is lower than the runoff from the Rhône basin (3.1 m yr^{-1}) we attribute the elevated cation flux from the Oberaar watershed primarily to the dissolution of approximately 6–7 times more calcium in this catchment (555 keq km^{-2} yr^{-1}, and 82–96 keq km^{-2} yr^{-1} of dissolved calcium are exported from the Oberaar and Rhône catchments respectively; i.e., 81% and 55% of the total cation flux). We attribute this difference in calcium flux to calcite concentrations which are on average 17.7 times higher in the Oberaar meltwaters, a 6 times greater flux of sulphate denuded from the Oberaar catchment and increased CO_2 draw down within the Oberaar catchment.

2. MATERIAL AND METHODS

2.1. Field Areas and Field Methods

This study focuses on the catchments of the Rhône and Oberaar glaciers, in the central part of Switzerland (Fig. 1). The present-day ice cover in the Rhône and Oberaar catchments is 73% and 57% respectively. The catchments are of comparable size, altitude, and climate (Table 1) and have a simple geometry with one focussed meltwater outlet. The geology of the catchments is similar, as they are both situated on the crystalline Aar massif, the bulk mineralogy of which

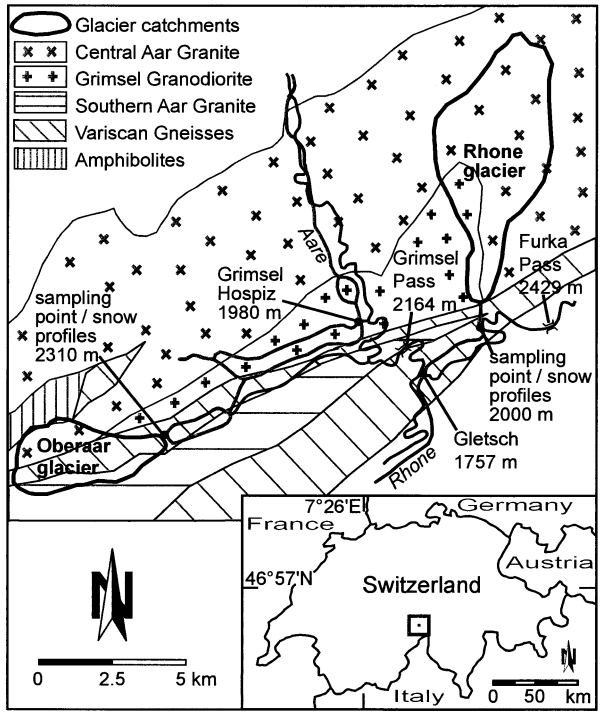

Fig. 1. The geography and geology of the field areas.

was analysed using optical microscopy, (Keusen et al., 1989 Table 2). The Rhône catchment is underlain by the Central Aar Granite, 90% and the Grimsel Granodiorite, 10%. The Oberaar watershed is centred on a strongly foliated gneissic zone, which represents 42% of the catchment area and contains up to 9% calcite (Arn, 2002). The sides of the catchment are made up of 38% Central Aar granite, 12% Southern Aar granite and 8% Grimsel granodiorite. (Stalder, 1964; Oberhänsli and Schenker, 1988 see Fig. 1 for a geological map).

Meltwater samples from the glaciers' outwash streams were collected on a daily basis during the 1999 and 2000 ablation periods. Samples were taken at minimum and maximum discharge (10:00 and 17:00 h; Gurnell et al., 1994). In 1999 sampling commenced on the 6th of July 1999, due to the late clearance of snow from the mountain

Table 1. A comparison of the catchments.

	Oberaar	Rhone
Geographical position	46° 32′ N 8° 14′ E	46° 35′ N 8° 23′ E
Surface of catchment	11.03 km^2	26.2 km^2
Altitude	2310–3631 m a.s.l.	1757–3630 m a.s.l.
Glacier cover today (%)	57%	73%
Annual mean temperature*	−1° C†	+1.2° C†
Annual mean precipitation*	2100 mm	2200 mm
Geology of field areas:		
Central Aar Granite	38%	90%
Grimsel Granodiorite	7%	10%
Variscan gneisses	42%	—
Ultramafic Inclusions	1%	—
Southern Aar Granite	12%	—

* Schwab et al. (2001).
† within proglacial area; 2300 m at Oberaar, 1757 m at Rhone.

Table 2. Mineralogical composition of the glacial suspended sediments and the bedrock (Central Aar Granite and Grimsel Granodiorite).

	n	Quartz	K-Feldspar (Microcline)	Plagioclase (Albite)	Calcite	Phyllosilicates[%]	Unquantifiable*	Epidote	Titantite
Rhône suspended sediment[§]	23	21.8 ± 6.9	17.2 ± 11.1	27.9 ± 16.7	0.5 ± 0.4	14.2 ± 10.8	23.7 ± 27.7		
Oberaar suspended sediment[§]	23	24.3 ± 13.5	6.5 ± 5.7	25.4 ± 11.5	2.3 ± 1.8	13.7 ± 5.5	28.5 ± 17.9		
Central Aar Granite[†]		32.4	33.0	20.9	<1	9.7		2.9	0.8
Grimsel Granodiorite[†]		28.3	24.4	29.1	<1	16.0		2.5	1.3

[§] Results from quantitative bulk rock XRD.

[†] Microscopical quantification (Keusen, 1989) converted to weight % using approximate mineral densities. Phyllosilicates are identified as biotite, chlorite and white mica. Apatite is reported at <1% in both lithologies.

* Minerals that cannot be quantified due to differences in chemical composition between samples and reference standards used, e.g. different Na: Ca ratios in the plagioclase feldspars.

[%] Individual phyllosilicates (e.g. phengite, biotite) cannot be quantified, as differences in their chemical composition affects their unit cell parameters.

passes. But discharge started to rise at the hydrographic station at Gletsch (Fig. 1) on the 1st of May 1999 and we interpret this as the start of the ablation period. We estimate that the ablation period ended on the 1st of November 1999. The discharge dropped below 1 $m^3\ s^{-1}$ at Gletsch on this date and continued to fall, with the first snowfall on the 7th of November 1999. In 2000 the discharge began to rise on the 20th of April 2000. Discharge dropped below 1 $m^3\ s^{-1}$ on the 8th of November 2000 and the regression continued from this date. The last of the winter's snow fell on the 25th of April 2000. We therefore consider the months May to October inclusively as the ablation period. Throughout the winters of 1999–2000 and 2000–2001 samples were taken on a monthly basis from October until April. On each sampling, 500 mL of meltwater was filtered immediately in the field, as recommended by Slatt (1972) using 0.45 μm cellulose nitrate filters and a Nalgene filter unit with a hand pump. Conductivity and pH were immediately determined on the filtered samples in the field, using a WTW Multiline P4 meter. In the Rhône catchment alkalinity was measured within 15 min of sampling during the 1999 ablation season, measurements were made on filtered meltwaters by titration with 0.1 mol/L, Titrisol HCl. HCO_3^- concentrations were also calculated as the difference between each sample's summed cation and anion concentrations. In both field areas, sample manipulations were performed in tents to limit contamination by dust or precipitation.

Snow samples were taken from 40–80 cm deep sample pits, dug in fresh snow in the pro-glacial areas of the two catchments during the accumulation periods. Rainwater samples were taken during the ablation periods: A polypropylene bottle was connected to a plastic funnel via a polypropylene tube and the bottle was left for a maximum of 24 h before the rainwater was filtered and stored. The funnel was protected from dust between samples by covering it with a plastic bag. All filtered samples were bottled in duplicate, kept in the dark at 2°C and analysed within 2 months. Samples intended for anion analysis were stored in polypropylene bottles, preleached with ultra-pure deionised water. Samples intended for cation analysis were stored in polypropylene bottles that had been preleached with 10% super-pure HNO_3 and then rinsed 3 times with ultra-pure deionised water. The sediment-laden filters were stored in individual Perspex boxes.

The atmospheric dust flux entering the Rhône catchment during the 1999 and 2000 ablation periods was measured using two 0.32 m diameter, 60 L plastic barrels, preleached with 10% super pure HNO_3 and thoroughly rinsed. The barrels were mounted in open, elevated positions, to avoid collecting saltating grains; a large flat-topped erratic boulder approximately half way up the glacier (barrel A) and a flat grassy step on the northerly side of the glacier snout (barrel B). Dust was prevented from being blown back out of the barrels by placing a 5 cm deep slatted container holding glass marbles at the mouth of the barrel (the marbles were cleaned in the same way as the barrel; Martin Reheis U.S. Geological Survey, pers. comm.). The barrels were left for 48 days in 1999 and 107 days in 2000 and then the contents were siphoned off and filtered through 0.45 μm filter papers, the barrels were thoroughly rinsed out with several washings of ultra-pure deionised water, which were also filtered.

2.2. Laboratory Methods

The major cations and anions Mg^{2+}, Ca^{2+}, K^+, Na^+ and SO_4^{2-}, NO_3^-, Cl^- were measured using ion chromatography (Dionex DX-500 equipped with CG/CS-12 and AG/AS-11HC columns, respectively). The precision is 5% for concentrations of $<$ 100 ppb and $\approx$ 2% for concentrations $>$ 100 ppb. Fe and Al were measured using a Zeeman graphite furnace AAS. The precision for Fe was 10% for concentrations of $<$ 15 ppb and 5% for concentrations of $>$ 15 ppb. The precision for Al was 20% for concentrations of $<$ 15 ppb, 10% for concentrations of 15–50 ppb, and 3% for concentrations of $>$ 50 ppb. Adsorbed cation concentrations were measured following Lorrain and Suchez (1972). The sediment-laden filters were washed three times with 10 mL 1N ammonium acetate (pH 7), pumping each aliquot through a Nalgene filter unit. The resultant combined leachate was filtered and analysed for Mg^{2+}, Ca^{2+}, Na^+ and K^+ using flame atomic absorption (Perkin Elmer 5100 PC). The blanks were 10 times lower than samples in each series, apart from the Rhône Ca^{2+} values and all the Na^+ values, which were the same as the blanks. Dissolved silicon was measured colorimetrically (molybdate blue) by FIA (tecator 5017) (modified from Mullin and Riley, 1955). The relative error for these two methods is $>$ 5%.

Filters were dried at 40° C, weighed and corrected for the original filter weight to calculate the mass of suspended sediment. The mineral content of the suspended sediment was determined by X-ray diffraction (XRD; Scintag XDS 2000), while the sediment was still on the filter papers (partial orientation). The dust samples were passed under the X-ray on silver-coated stubs. The bulk mineralogy of the suspended sediments was determined by semiquantitative analysis using external standards (Adatte et al., 1996). The limit of detection for calcite is 0.2%. Un-orientated powder samples have an error of 5% and we estimate that our partially orientated powder samples have an error of $<$ 10%. The granulometry of the suspended sediment and dust samples was determined using a Laser Oriel granulometer. The chemistry of the suspended sediment was determined by XRF, at the University of Fribourg, using a sequential X-ray spectrophotometer (PW-2400), with a relative error of 0.2–1% for major elements.

2.3. Precipitation Input Corrections

We calculate the input flux for wet precipitation in two ways: firstly by correcting each meltwater sample for precipitation inputs in proportion to its chloride concentration and secondly based on the estimated volumes of rain and snow falling in the catchments.

In the first approach, the concentration of ions in each meltwater sample, X_m are corrected, to give the weathering derived concentrations in the meltwaters, X^*_m. The relative input of ions by wet precipitation is calculated by multiplying the chloride concentration in the meltwaters Cl_m by the mean concentration of each ion in precipitation X_p and dividing by the mean chloride concentration of the precipitation:

$$X_m^* = X_m - Cl_m \cdot X_p/Cl_p$$

Table 3. Precipitation compositions in μeq l^{-1}.

Sample	Date(s)	Na^+	K^+	Mg^{2+}	Ca^{2+}	Fe^{3+}	Al^{3+}	Cl^-	SO_4^{2-}	NO_3^-	NH_4	Si
Rain												
Rh	28-Aug-99	8.70	7.16	5.76	43.91	n.a.	n.a.	5.64	54.76	15.64	n.a.	n.a.
Rh	7-Sep-99	10.87	6.14	4.11	33.43	1.51	1.68	3.67	33.31	28.22	n.a.	6.61
Rh	22-Sep-99	4.78	2.05	1.65	2.50	1.99	2.36	1.41	5.41	5.32	n.a.	n.a.
Rh	31-May-00	2.15	1.52	0.00	5.17	0.09	1.01	1.69	7.29	9.84	n.a.	0.57
Rh	7-Jun-00	4.03	6.16	1.31	23.29	0.05	0.61	4.23	28.11	32.42	n.a.	8.29
Rh	28-Jun-00	5.96	5.19	4.62	21.41			4.23	24.36	23.39		
Ob	11-Jul-00	16.96	3.58	10.70	134.23	0.12	0.38	3.10	12.91	10.97	n.a.	52.74
Ob	13-Jul-00	2.75	1.28	0.00	8.37	0.56	0.79	2.26	50.59	5.00	n.a.	64.06
Rh	15-Jul-01	n.a.	2.30	2.47	10.98	0.14	0.86	4.22	29.72	17.61	n.a.	n.a.
Rh	27-Jul-00	3.57	1.84	1.56	5.25	0.62	0.87	3.10	20.40	16.93	n.a.	n.a.
Rh	1-Aug-00	3.09	2.27	0.59	3.10	0.60	0.61	5.36	16.24	13.22	n.a.	1.81
Rh	7-Aug-00	2.47	1.51	1.37	16.76			1.68	19.57	17.10		
Rh	3-Aug-01	2.61	3.07	1.65	7.49	0.33	n.a.	1.94	12.59	6.44	n.a.	n.a.
Ob	3-Aug-01	3.04	4.35	2.47	17.47	0.18	n.a.	3.80	38.18	21.58	n.a.	n.a.
Ob	8-Aug-01	2.61	7.67	1.65	11.48	0.05	0.77	3.74	15.84	14.18	n.a.	n.a.
Rh	17-Aug-01	4.35	9.21	4.11	25.95	0.14	1.11	6.21	19.52	18.01	n.a.	n.a.
Rh	30-Aug-01	6.09	8.18	6.58	53.39	n.a.	0.88	8.46	17.08	19.97	n.a.	n.a.
Snow (sample depth)												
$Rh_{(0–85\ cm)}$	18-Jan-01	6.52	2.30	0.82	2.00	0.28	1.05	n.a.	n.a.	n.a.	n.a.	2.87
$Ob_{(0–5\ cm)}$	18-Jan-01	5.22	8.16	0.38	4.00	0.30	1.27	9.87	2.58	3.85	n.a.	0.45
$Ob_{(0–40\ cm)}$	6-Mar-01	2.75	2.57	0.47	16.96	n.a.	n.a.	5.36	2.07	3.60	n.a.	n.a.
$Ob_{(0–5\ cm)}$	6-Mar-01	2.45	1.88	0.29	14.31	b.d.	0.80	2.81	2.30	2.94	n.a.	n.a.
$Rh_{(0–5\ cm)}$	7-Mar-01	0.29	0.99	0.00	1.42	n.a.	n.a.	n.a.	n.a.	n.a.	n.a.	
Mean Rain	1999–2001	4.47	4.37	2.49	18.12	0.52	1.05	3.85	24.56	16.55	—	11.62
Mean Snow	1999–2001	3.45	3.18	0.39	7.74	0.19	1.04	5.14	2.54	4.87	—	0.83
Average (ratio 40:60)		3.86	3.65	1.23	11.89	0.33	1.04	4.63	11.35	9.54	—	5.15
Cl/ion		0.83	0.79	0.27	2.57	0.07	0.23	1.00	2.45	2.06	—	1.11
Sea Salt (Cl/ion)		0.56	0.20	0.07	0.20	—	—	—	0.14	—	—	—
Other swiss sites												
Alptal (annual mean)[†]		5.65	1.28	1.65	12.48	0.59	0.56	4.51	6.25	4.19	0.01	7.12
Haut Glacier d'Arolla*	1993-1995	0.40	1.10	0.70	3.80	n.a.	n.a.	3.80	3.30	5.80	n.a.	<0.1

n.a.: not analysed, b.d.: below detection.
* Rain collected during Saharan red dust event and not included in the mean.
[†] non glaciated; average annual precipitation 2300 mm (P Schleppi, pers. comm.).
[#] Mean snowpack winters 93–95, Tranter et al. (2002).

Between August 1999 and September 2001, 17 rain and 5 snow samples were collected and used to determine the mean rain and snow concentrations (Table 3). These means are weighted according to the relative proportions of rain and snowfall (in water equivalents) recorded at the Grimsel Hospiz during the study period (60% snow: 40% rain; MeteoSuisse; station 5010), yielding a mean annual precipitation composition (Table 3). The Hospiz is located at 1980 m, on the northerly side of the Grimsel Pass, approximately 4 km from the Rhône and 8 km from the Oberaar glacier snouts (Fig. 1.) and provides a daily record of precipitation volumes. Regarding the second volumetric approach mean annual precipitation data at the Hospiz for 1997, 1999 and 2000 average 2040 mm per year, slightly higher than the average precipitation rate from 1988–2000:1990 mm. Precipitation was assumed to fall as snow from November to April yielding an average snow/total precipitation ratio of 0.68 for September 1999–2000 and 0.53 for September 2000–2001. In the Rhône catchment Bernath (1991) recorded annual inputs ranging between 2108–2845 mm for the period 1979–1983, based on a detailed net of climatological stations. Estimates based on a 20-yr local climate record (1971–1990) give an average of 2050 mm of precipitation (Schwab et al., 2001). Because a slightly higher than average precipitation volume is recorded at the Hospiz during our study period we estimate an annual precipitation input of 2200 mm in the Rhône catchment with 60% of this volume falling as snow. In the Oberaar catchment an annual mean precipitation of 2020 mm has been observed (Schwab et al., 2001). Again, to reflect the elevated precipitation volume recorded at the Hospiz, we use a slightly higher value: 2100 mm, with snowfall representing 60% of this volume. These rain and snow volumes are multiplied by the mean rain and snow composition to calculate the wet precipitation input to each catchment, which is subtracted from the meltwater fluxes to obtain a denudation rate.

All ion corrections are subject to some error, firstly because we use mean rain and snow composition, whereas ion concentrations vary significantly during individual rain events (Table 3) and secondly because ions are eluted at different rates from the snow pack, leading to a non-linear relationship between Cl^- and other ions at the start of the ablation season. Both correction methods fail to remove approximately half the NO_3^- flux (Table 4), but correction for NO_3^- may be especially difficult, for example because NO_3^- may be influenced by subglacial microbial activity (Sharp et al., 1999) and NH_4^+ in rain. The volumetric correction overestimates the total precipitation volume, as negative Cl^- fluxes are calculated (Table 4). We therefore use precipitation ratio values in the discussion section of this paper, and point out that this approach is certainly more robust than using sea salt ratios for catchments located in the continental interior (Table 3).

2.4. Flux Calculations

Rhône daily discharges for the 1999 and 2000 ablation periods were recalculated from Swiss National Hydrological Survey data (Federal Office for Water and Geology) from the Gletsch gauging station (no. 2268). The gauging station is 2.75 km downstream from the glacier snout and receives water from a 38.9 km^2 catchment. Bernath (1991) made a detailed 5-yr hydrological study of the Gletsch catchment and calculated that between 14 and 18% of the discharge measured at Gletsch comes from outside the Rhône glacier catchment. We calculate all our ablation period daily fluxes based on the Gletsch daily discharge measurements corrected by 14 and 18% and mean daily meltwater

Table 4. Annual dissolved fluxes from the catchments (keq km^{-2} $year^{-1}$) and suspended sediment fluxes (t km^{-2} $year^{-1}$).

	Ca^{2+}	K^+	Na^+	Mg^{2+}	Fe^{3+}	Al^{3+}	Cl^-	SO_4^{2-}	NO_3^-	HCO_3^-*	Si	Suspended Sediment
Uncorrected fluxes												
Rhone	96.4/116.2	29/35.4	28.3/34.1	14.9/18.1	5.4/6.5	11.0/13.3	6.6/8.2	49.9/60.0	34.2/42.5	82.2/106.2	152.3/183.2	388/491
Oberaar	589.5	59.7	32.4	37.0	4.8	10.4	5.9	226.8	23.8	467.2	182.2	773
Corrected by precipitation volumes												
Rhone	70.2/90.0	21.0/27.4	19.8/25.6	12.2/15.4	4.7/5.8	8.7/11.0	−2/−3.6	24.9/35.0	—	—	141.0/171.9	
Oberaar	564.5	52.0	24.3	34.4	4.1	8.2	−3.8	203.0	—	—	171.4	
Corrected by precipitation ratios												
Rhone	81.5/96.4	24.5/29.3	23.1/27.3	13.6/16.4	2.2/2.7	2.1/2.6	0	33.7/39.3	20.5/24.7	93.2/109.7	145.3/173.2	
Oberaar	554.6	53.3	26.1	33.9	4.4	8.9	0	204.5	11.8	467.6	176.4	

* HCO_3^- concentrations are calculated to bring the uncorrected and precipitation corrected meltwaters to a charge of 0.

concentrations to show the discharge related error on our values. Accumulation period discharges are based on visual estimates and agree well with those proposed by Bernath (1991).

Oberaar discharges were estimated visually to the nearest 0.5 m^3 s^{-1} each time a meltwater sample was taken, based on estimated water velocity and channel geometry. The meltwater channel was relatively stable. The accuracy of these estimates was compared with discharges calculated using the salt dilution method (Federal Office for Water and Geology, 1994). Discharge estimates of 1.5 m^3 s^{-1} were calculated as 1.64, 1.58 and 1.41 m^3 s^{-1} on three separate occasions using salt dilution. The calculated mean monthly discharges for the Oberaar stream based on these regular estimates agrees well with the mean monthly discharge estimates produced using a model designed by the Swiss National Hydrological Survey, Federal Office for Water and Geology. Fluxes are calculated for each sample as the product of the ion or suspended sediment concentration and the discharge volume. The mean of the 10:00 and the 17:00 h fluxes is taken to represent the daily flux. In both catchments the daily fluxes are used to calculate monthly fluxes, which are summed to give yearly fluxes. Fluxes are normalised by catchment area allowing comparison between catchments. Linear regressions between discharges measured at Gletsch at 10:00 and 17:00 and corresponding ion concentrations (Sharp et al., 1995) show no significant correlation, therefore we do not calculate hourly fluxes based on regression models.

To calculate adsorbed cation fluxes the adsorbed cation concentrations from 10:00 and 17:00 h samples for each day were averaged to calculate a daily mean adsorbed concentrations (mg g^{-1}). Weighted monthly concentrations were averaged to calculate a mean annual adsorbed cation concentration (mg g^{-1}), which was multiplied by the annual sediment flux to obtain an annual adsorbed cation flux.

3. RESULTS

3.1. Atmospheric Dust Flux

In 1999 the mean daily dust input up to barrel A was of 13.7 mg m^{-2} day^{-1}. Unfortunately barrel B was lost. In 2000 barrel A recorded a mean daily dust input of 16.2 mg m^{-2} day^{-1} and barrel B recorded 18.7 mg m^{-2} day^{-1}. This implies that dust fall is evenly spread over the glacier. The annual dust input is therefore approximately 5.9 t km^{-2} yr^{-1}, or 1% of the suspended sediment flux (see below). Dust samples contained quartz, mica, chlorite, potassium and plagioclase feldspars, goethite, calcite, smectite and kaolinite. In 1999 a red fraction was observed in the generally grey coloured dust. Red coloured dust was also collected during a rain event in 2000. The red colour of some of the dust and the presence of kaolinite suggests that a component of the dust is not local. It maybe of Saharan provenance (Lenaz et al., 1986; Kübler et al., 1990), although dolomite, another mineral typical of peridesertic environments, is not observed. It may have dissolved in the barrels before the sediment was filtered.

3.2. Suspended Sediment

The annual variation in the 10:00 and 17:00 h suspended sediment concentrations in the meltwaters of the two catchments and the daily mean discharge recorded at Gletsch are plotted in Figure 2a. Suspended sediment concentrations in the Oberaar meltwaters are consistently higher than in the Rhône meltwaters. The mean ablation period concentration are 0.11 g l^{-1} (± 0.05; n=196; Rhône) and 0.33 g l^{-1} (± 0.10; n=107; Oberaar). The average winter suspended sediment concentrations are lower, 0.03 g l^{-1} (± 0.02; n=6;Rhône) and 0.04 g l^{-1} (± 0.03; n=6; Oberaar). Figure 2a also shows that high discharges, associated with the rapid melting of snow and heavy rain events provoke the evacuation of large volumes of sediment. In both catchments, rain events, coinciding with the snow melt period, mobilise large volumes of sediment. For example 3% of the annual sediment yield was discharged from each catchment during the rainstorm on the 6th of July 1999. The highest Rhône suspended sediment concentrations are associated with a two day rain event on the 20th and 21st of September 1999. The event was of a magnitude that only occurs once every 2.3 yr (Schwab et al., 2001) and the sediment exported during these two days represents 9% of the annual suspended sediment flux. This event was not recorded in the Oberaar catchment. The main flushing events in both catchments occurred when a distributed, rather than a channalised, drainage system predominated, thus creating a larger interface between subglacial sediment and meltwaters (e.g., Nienow et al., 1996).

The suspended sediments of the two catchments contain quartz, plagioclase, alkali feldspar, phyllosilicates and calcite (XRD values). In addition some of the Oberaar samples contain amphibole. The bulk mineralogical analysis shows that the quartz, plagioclase feldspar and phyllosilicate content of suspended sediments in the two catchments are similar, but that the Oberaar suspension contains less potassium feldspar than the Rhône suspension. The phyllosilicates have been identified as biotite, phengite and chlorite (Keusen, 1989). The mean calcite concentration is significantly higher in the Oberaar suspension than in the Rhône (2.3% and 0.5% respectively, Table 2). The mean Na_2O and SiO_2 concentrations of the suspended sediments are similar (XRF, Rhône and Oberaar Na_2O; 3.8 & 3.0%

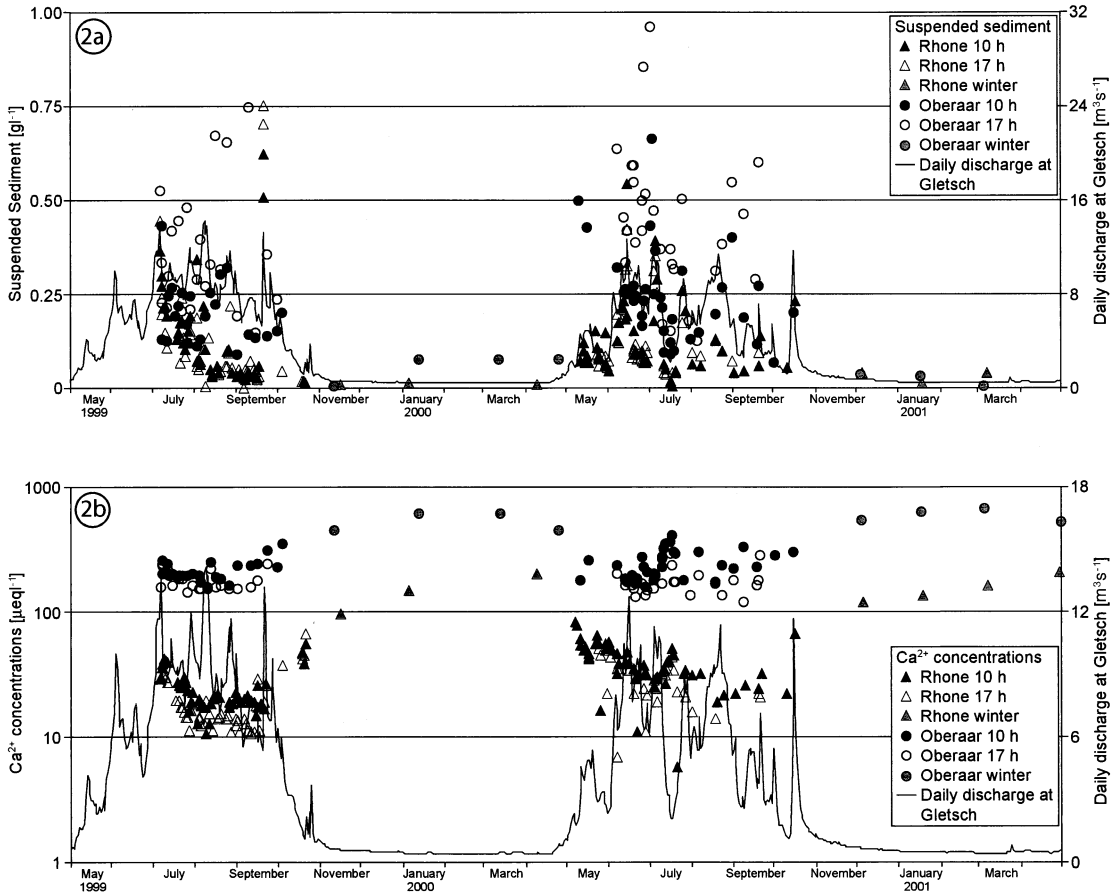

Fig. 2. Ca^{2+} and suspended sediment concentration.

respectively; Rhône and Oberaar SiO_2; 68% & 63% respectively). The mean CaO content of the Rhône suspended sediment is approximately half that of the Oberaar suspended sediment (0.9% & 2.0%, respectively). The strontium and barium concentrations are observed to be elevated in the Oberaar suspended sediments (Ba: 982 ppm, Sr: 238 ppm) with respect to the Rhône (Ba: 524 ppm Sr: 102). The oxides of titanium and phosphorus that are found in granitic rocks associated with minerals that contain calcium (sphene and apatite respectively) are also more prevalent in the Oberaar catchment (TiO_2 = 0.66%, Oberaar & 0.4%, Rhône; P_2O_5 = 0.18%, Oberaar & 0.1% Rhône). Ferric iron concentrations are also elevated in the Rhône sediments (Oberaar = 3.2%; Rhône = 1.8%) indicating a higher concentration of iron sulphides in the Oberaar catchment.

In the two catchments the suspended sediment has a modal grain size in the 4–8 μm range, with 33% of the sediment in this size fraction. The suspended sediment flux from the Oberaar catchment is 773 t km^{-2} yr^{-1}, whereas in the Rhône catchment it is 388–490 t km^{-2} yr^{-1}.

3.3. Wet Precipitation Composition

Mean rain and snow chemistries are listed in Table 3; we also list average annual precipitation concentrations for the Alptal (P Schleppi, personal communication). This non-glaciated valley lies at the northern edge of the Swiss Alps, approximately 80 km from our field areas, between 1100 and 1600 m altitude. Our average annual concentrations agree well with the Alptal dataset, i.e., within 2–3 μeq l^{-1}, the exceptions being the SO_4^{2-} and NO_3^- concentrations, which are approximately twice as high in our glacial catchments. SO_4^{2-} and NO_3^- concentrations in snow agree well with the data for the Haut Glacier d'Arolla (Tranter et al., 2002).

3.4. Meltwater Composition

Calcium dominates the meltwater chemistry of the Oberaar watershed and is the second most important ion after silica in the Rhône watershed (Table 5). Figure 2b shows meltwater samples taken at 10:00 h have higher Ca^{2+} concentrations than the corresponding samples taken at 17:00 h. Mean Ca^{2+} concentrations are higher during the accumulation period (Rhône Ca^{2+} concentrations = 4.5 × higher and Oberaar Ca^{2+} concentrations = 2.6 × higher; see Table 5), when discharge is 0.1– 0.3 m^3 s^{-1}, than during the ablation period, when average monthly discharge ranges from 1– 10 m^3 s^{-1}. These trends observed for Ca^{2+} are representative for the other dissolved ions. Oberaar meltwater Ca^{2+} concentrations are an order of magnitude higher than Rhône meltwater ones during the 1999 and 2000 ablation periods (Fig. 2b) and Oberaar accumulation period samples contain approximately four times as much Ca^{2+}

Table 5. Monthly averages* have been calculated from daily (10:00 & 17:00) measurements from 1999 to 2001 (see also Fig. 2).

	n	Na^+	±	K^+	±	Mg^{2+}	±	Ca^{2+}	±	Fe^{3+}	±	Al^{3+}	±	Cl^-	±	SO_4^{2-}	±	NO_3^-	±	†HCO_3^-	±	††HCO_3^-	±	Si	±	Cond.	±	pH	±	SI (calcite)	Disch.#	Model§
Rhone																																
January	1	44.3	—	32.7	—	20.8	—	147.7	—	2.8	—	5.9	—	3.9	—	98.5	—	22.3	—	129.6	—	n.a.	—	263.3	—	25.5	1.4	7.32	0.01	2.4E-04	0.20	0.06
March	1	47.8	—	35.0	—	20.6	—	163.2	—	n.a.	—	n.a.	—	n.a.	—	n.a.	—	n.a.	—	n.a.	—	n.a.	—	n.a.	—	15.0	—	7.40	—	n.a.	0.20	0.06
April	1	40.2	—	33.1	—	19.3	—	206.3	—	0.7	—	1.6	—	3.4	—	95.6	—	15.7	—	186.5	—	n.a.	—	230.7	18.8	16.3	—	7.86	—	1.7E-02	0.20	0.16
May	16	15.4	4.0	15.2	3.5	8.0	3.0	53.6	13.1	1.2	0.2	1.7	0.5	3.7	0.8	26.1	13.0	19.9	2.8	45.7	14.6	n.a.	—	57.0	19.1	12.5	5.15	6.58	0.39	5.7E-05	0.30	0.95
June	9	10.4	2.9	12.3	4.9	5.2	1.3	34.2	8.4	1.1	0.4	1.3	0.4	2.5	0.4	17.0	3.6	15.5	2.8	30.1	11.1	n.a.	—	34.8	16.7	8.7	1.87	6.23	0.29	1.0E-05	2.27	3.80
July	25	7.8	2.8	8.3	2.1	4.1	1.7	27.3	8.1	1.0	0.4	1.2	0.5	2.3	0.6	14.1	4.0	12.6	3.2	21.3	10.4	16.3	13.2	33.5	8.7	8.1	2.3	6.16	0.33	5.1E-06	5.52	6.12
August	9	5.0	0.8	6.1	1.6	3.7	4.7	17.2	2.6	0.7	0.5	0.7	0.6	1.7	0.6	9.4	2.4	8.5	2.4	15.5	6.02	12.3	20.6	22.1	7.4	7.2	4.9	5.77	0.26	8.8E-07	7.14	5.95
September	9	5.6	4.8	7.5	5.0	3.4	1.1	18.8	4.7	1.1	0.7	1.5	0.8	1.5	0.3	7.8	1.9	6.0	1.0	24.7	14.4	16.8	18.4	25.5	13.7	5.3	1.6	5.70	0.27	1.3E-06	7.79	3.45
October	3	14.0	2.0	14.0	4.2	7.0	3.3	51.8	12.9	1.4	0.4	2.2	0.4	2.6	0.5	24.8	4.6	13.3	2.8	50.0	14.7	25.5	8.9	103.8	65.8	9.9	1.4	6.39	0.26	3.4E-05	4.14	1.04
November	1	26.2	—	20.8	—	12.7	—	96.0	—	1.2	—	2.4	—	3.4	—	45.4	—	17.6	—	92.9	—	20.0	—	147.9	—	18.0	—	7.50	—	1.7E-03	1.97	0.20
December	1	35.2	—	26.6	—	16.5	—	120.8	—	0.6	—	1.3	—	5.0	—	59.6	—	20.0	—	116.4	—	n.a.		250.7	—	47.0	—	6.91	—	7.0E-04	0.40	0.09
Oberaar																																
January	2	42.5	3.2	64.1	1.6	36.6	2.9	616.9	13.9	0.7	0.0	3.9	0.9	2.7	1.0	395.1	26.9	10.6	5.6	356.5	42.9			180.8	—	86.3	1.2	7.47	0.31	4.0E-02	0.10	0.05
March	2	47.1	1.1	61.6	6.5	39.9	6.4	645.2	38.8	0.5	0.1	3.0	0.2	3.0	0.2	300.8	33.0	11.7	3.1	481.9	88.6			n.a.	—	90.0	2.8	7.65	0.10	1.9E-09	0.10	0.05
April	2	39.0	7.6	48.1	5.5	30.9	5.1	484.5	50.1	1.3	0.9	3.5	1.0	4.4	1.7	140.3	149.2	21.2	4.7	441.4	76.3			193.7	18.22	67.5	7.7	7.86	—	5.9E-02	0.25	0.09
May	2	16.0	0.2	26.2	4.9	16.1	3.6	218.0	55.8	2.4	2.2	4.3	3.1	3.4	1.2	54.5	38.3	17.5	6.7	207.6	39.4			113.6	16.46	29.0	5.7	7.60	0.07	2.0E-02	0.63	0.83
June	11	9.1	1.6	16.7	1.9	10.9	2.2	179.9	23.9	2.3	0.6	3.9	0.7	2.2	0.2	62.9	10.4	10.6	2.6	147.1	17.3			55.8	8.769	23.3	2.3	7.35	0.10	6.5E-03	1.70	1.69
July	10	11.0	4.3	21.5	5.5	14.4	3.3	221.1	49.8	1.9	0.9	4.0	1.4	2.2	0.4	92.2	25.5	10.5	3.0	168.9	51.4			62.5	24.7	29.4	6.9	7.47	0.40	5.0E-03	2.11	2.35
August	10	7.6	1.8	17.5	3.4	11.3	2.5	185.3	31.4	2.2	0.9	4.4	1.4	2.0	0.1	66.4	14.6	6.2	1.3	153.8	25.3			62.0	39.3	25.2	4.6	7.42	0.40	5.0E-03	1.98	2.15
September	8	7.8	3.6	20.3	7.0	13.2	4.5	191.6	63.3	2.1	0.8	4.6	1.4	2.4	0.7	80.6	15.8	6.2	1.8	150.5	64.7			56.4	15.6	30.0	5.4	7.40	0.40	4.6E-03	1.86	1.51
October	3	16.8	0.6	33.4	2.3	19.6	4.6	313.3	39.3	2.2	2.1	5.3	3.2	3.0	0.8	113.0	51.7	12.6	3.2	262.0	33.4			74.9	52.3	39.9	10.2	7.11	0.10	1.3E-02	0.75	0.39
November	1	31.2	—	54.6	—	31.2	—	456.4	—	3.1	—	6.6	—	2.3	—	252.6	—	14.0	—	314.3	—			n.a.	—	64.7	—	7.72	—	1.1E-02	0.25	0.11
December	1	33.9	—	60.8	—	33.7	—	547.9	—	0.9	—	3.1	—	3.2	—	312.8	—	15.0	—	349.2	—			n.a.	—	76.6	—	7.84	—	6.2E-02	0.20	0.05

* Ionic concentrations in μeq1^{-1}; conductivities in μS cm^{-1}; discharge in m^{-3} s^{-1} & PCO_2 in atm. Values are not corrected for precipitation inputs.
n.a. not analysed.
§ Modelled discharge; Swiss National Hydrological Survey (Federal Office for Water and Geology), see text.
† Calculated HCO_3^-
†† HCO_3^- measured during the 1999 field season.
# Rhone discharge measured at Gletsch by the Swiss National Hydrological Survey (Federal Office for Water and Geology); Oberaar discharge estimated, see text.

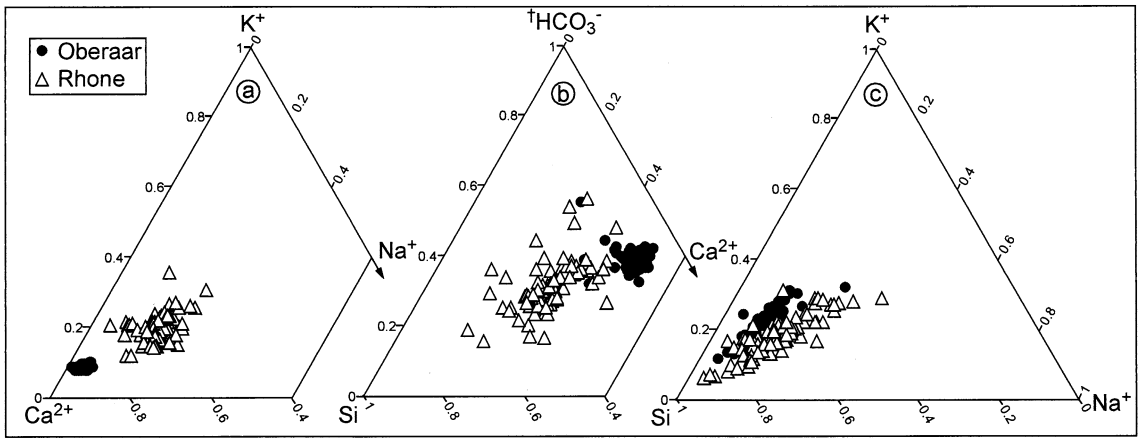

Fig. 3. Ternary diagrams of ions dissolved in meltwaters. ($^{\dagger}HCO_3^-$ = calculated HCO_3^-.)

as equivalent Rhône samples. This is reflected in the higher mean pH of the Oberaar meltwaters (7.40) compared to the Rhône meltwaters (5.97). The Oberaar meltwaters also have higher K^+, Mg^{2+}, SO_4^{2-} and calculated HCO_3^- concentrations than the Rhône meltwaters whereas the Na^+, Cl^-, NO_3^- and Si concentrations are comparable between the two areas (Table 5). The Rhône calculated and measured HCO_3^- concentrations fall within the same order of magnitude (Table 5), although the very dilute nature of the Rhône meltwaters appears to lead to an underestimation of their HCO_3^- content using the titrimetric method.

Two ternary diagrams show that the Oberaar meltwater compositions plot as a discrete population relative to the Rhône meltwater composition: In the Ca^{2+}-K^+-Na^+ ternary diagram the Oberaar samples are tightly grouped and plot much closer to the Ca^{2+} pole than the Rhône samples (Fig. 3a). Similarly in the Si-calculated-HCO_3–Ca^{2+} diagram the Oberaar samples plot closer to the Ca-HCO_3 boundary, whereas silica dominates over HCO_3^- and Ca^{2+} in most of the Rhône meltwater samples (Fig. 3b).

3.5. Fluxes

The precipitation ratio corrected Ca^{2+}, K^+, Mg^{2+}, calculated HCO_3^- and SO_4^{2-} fluxes calculated for the Oberaar catchment are elevated compared to those calculated for the Rhône (Ca^{2+} by 6–7 times; K^+ by 2 times; Mg^{2+} by 2; HCO_3^- by 5 times and SO_4^{2-} by 6 times; Table 4). The ranges reflect the possible errors in the Rhône fluxes due to the calculated discharge. The Na^+ and Si fluxes from the two watersheds are comparable. The trend in the mean monthly Ca^{2+} flux is representative for all the dissolved ionic fluxes (Fig. 4). Note ablation period Ca^{2+} fluxes are 3–4 times higher than accumulation period Ca^{2+} fluxes.

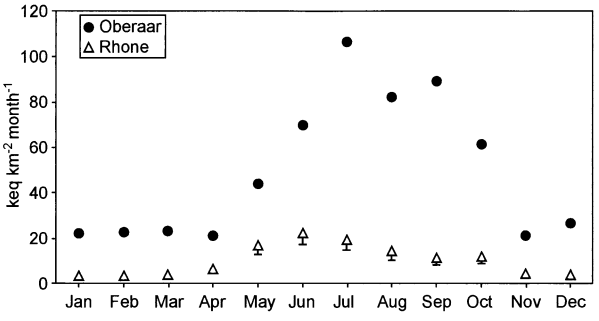

Fig. 4. Mean monthly Ca^{2+} fluxes from the two glaciers (1999–2001).

3.6. Adsorbed Cations

Average summer and winter adsorbed cation concentrations and annual adsorbed fluxes are shown in Table 6. Summer concentrations are higher than winter concentrations and the Oberaar annual adsorbed Ca flux is at least 4 times higher than the Rhône's. The adsorbed fluxes represent between 2% and 10% of the dissolved flux. These values are comparable with those of Lorrain and Souchez (1972).

4. DISCUSSION

4.1. Carbonate Dissolution

Many authors have observed the dominance of the calcium ion in glacial meltwaters draining crystalline catchments (e.g.,

Table 6. Adsorbed cation composition and fluxes.

	Ca^{2+}	K^+	Mg^{2+}
Oberaar			
mean ablation season (μeq g^{-1})	82.34 ($\pm$45.91)	2.05 ($\pm$1.79)	2.47 ($\pm$0.82)
mean accumulation season (μeq g^{-1})	27.49	1.46	0.95
keq km^{-2} yr^{-1}	40	1	1
Rhône			
mean ablation season (μeq g^{-1})	<23.95 ($\pm$19.96)*	5.88 ($\pm$8.44)	2.47 ($\pm$0.82)
mean accumulation season (μeq g^{-1})	<16.97	3.36	1.25
keq km^{-2} yr^{-1}	<8–10	2	1

* Although the blank was as high as the Rhône samples we show the calculated values to indicate the maximum possible fluxes.

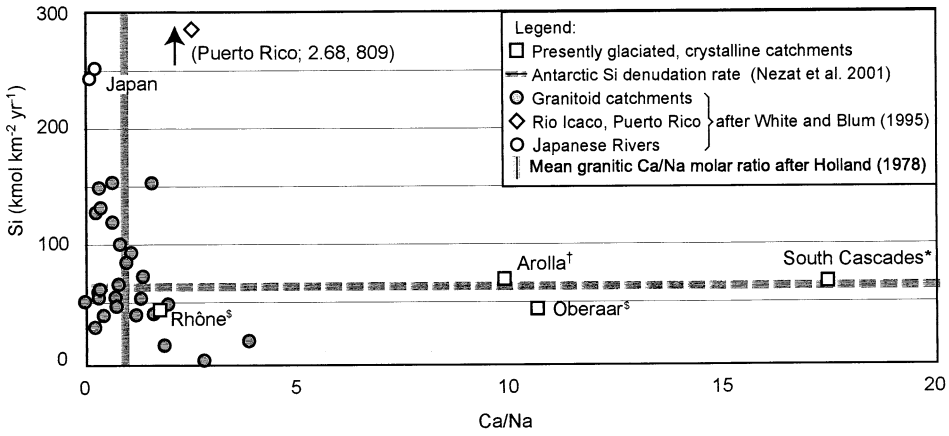

Fig. 5. Silicate and carbonate weathering in presently glaciated and non-glaciated granitoid catchments. All fluxes are corrected for precipitation inputs: †Sharp et al. (1995), *Axtmann and Stallard (1995) and $this study, cyclical salt corrections; White and Blum (1995), volumetric correction.

Eyles et al., 1982; Drever and Hurcomb, 1986; Anderson et al., 1997, 2000; West et al., 2002). Calcium also dominates our glacial runoff, which equally denudes crystalline watersheds, but 6–7 times more calcium is weathered from the Oberaar catchment compared to the Rhône (Table 4). The Oberaar's elevated calcium flux cannot be due to increased plagioclase dissolution nor due to other Ca-bearing minerals such as amphibole, sphene, epidote or apatite (see below). The most likely source of calcium is the increased calcite content of the Oberaar bedrock. The fine grain size of calcite in our catchments (modal grain size of the suspended sediment, 4–8 μm; with a tendency for calcite to be concentrated in the finer size fractions, Fairchild et al., 1999) renders it highly reactive in dilute meltwaters. XRD bulk mineralogy shows that the percentage of calcite is approximately 4.6 times higher in the suspended sediment exported from the Oberaar catchment compared to the Rhône (Table 2). The mean concentration of the suspended sediment in the Oberaar meltwaters is 0.31 g l^{-1} (the mean of accumulation and ablation period average concentrations) whereas the average concentration of suspended sediment in the Rhône meltwaters is 0.07 g l^{-1}. So the mean calcite content of the Oberaar meltwaters is 17.7 times greater than that of the Rhône meltwaters (7.1 mg l^{-1} and 0.4 mg l^{-1} of calcite, respectively). The total flux of calcium transported as calcite in the Oberaar meltwaters (7 t km^{-2} yr^{-1}) is 7 times higher than that transported by the Rhône meltwaters (1 t km^{-2} yr^{-1}). Since both the calcite content of the bedrock and the susceptibility to mechanical erosion are reflected in the flux of suspended calcite, we suggest that the latter can be used as a proxy for the total weathering surface area of calcite (in the suspended load and in the subglacial sediments). The flux of dissolved Ca^{2+} from the Oberaar catchment is six to seven times greater than that from the Rhône catchment it appears, therefore, that the Ca^{2+} flux scales in proportion to the mass of calcite (in the form of both suspended and subglacial sediment) in contact of the meltwaters of these two catchments. Similarly, the K^+ flux appears to scale in proportion to flux of suspended phyllosilicates. (Vermiculatisation of micas leads to the preferential release of K^+ ions into glacial waters; Drever and Hurcomb, 1986; Anderson et al., 1997). The Oberaar's K^+ flux is double the Rhône's (Table 4; Fig. 3c) as is the Oberaar's suspended sediment flux (Oberaar = 773 t km^{-2} yr^{-1}; Rhône = 388–490 t km^{-2} yr^{-1}; the phyllosilicate content of the suspended sediments is comparable).

The Oberaar's elevated Ca^{2+} flux cannot be due to increased plagioclase weathering, given that the suspended sediments from the two catchments contain very similar concentrations of albite (Table 2; XRF measurements) and the dissolved Na^+ fluxes from the two catchments are comparable (Table 4). Figure 5 compares the Ca/Na ratios in runoff from presently glacier-covered and non-glacier covered catchments with granitoid bedrock. The Rhône catchment plots within the scatter of non-glaciated catchments, whereas the Oberaar catchment plots with other glacierised catchments. The Ca^{2+}/Na^+ molar ratio in the Oberaar waters is 11, whereas it is 2 in the Rhône.

Amphibole was detected in some Oberaar suspended sediment samples, whereas it was not detected in the Rhône catchment: Stalder (1964) describes amphibolite lenses bordering the Oberaar catchment (Fig. 1; an actinolite composistion is likely; O. Müntener Neuchâtel, pers. comm.). However three points suggest that amphibole may be a minor source of calcium in the Oberaar catchment compared to calcite. Firstly the amphibole peak (XRD) is less than that of calcite, implying that it is present at concentrations of $< 1\%$, exact quantification is not possible using this method. Secondly the weathering rate of amphibole ($\approx 10^{-15}$ mol m^{-2} s^{-1}; Brantley and Chen, 1995) is ten orders of magnitude lower than that of calcite at near neutral pH and thirdly the magnesium fluxes from the two catchments are of the same order of magnitude (12.4–15.4 & 34.4 keq km^{-2} yr^{-1}; Rhône and Oberaar respectively).

The calcium bearing minerals apatite, epidote and sphene were also detected in both field areas (Keusen, 1989). Apatite dissolution is unlikely to augment the Oberaar Ca^{2+} flux, because orthophosphate concentrations are similar in the meltwaters of the two catchments (Hosein, 2002) and apatite weathering is minimal at near neutral pH (Stumm and Morgan, 1996). The influence of sphene on the meltwater composition is assumed to be negligible, as sphene is considered to be a recalcitrant mineral (e.g., Taylor and Blum, 1995 the weight percent of TiO_2 is 1.65 greater in the suspended sediment from

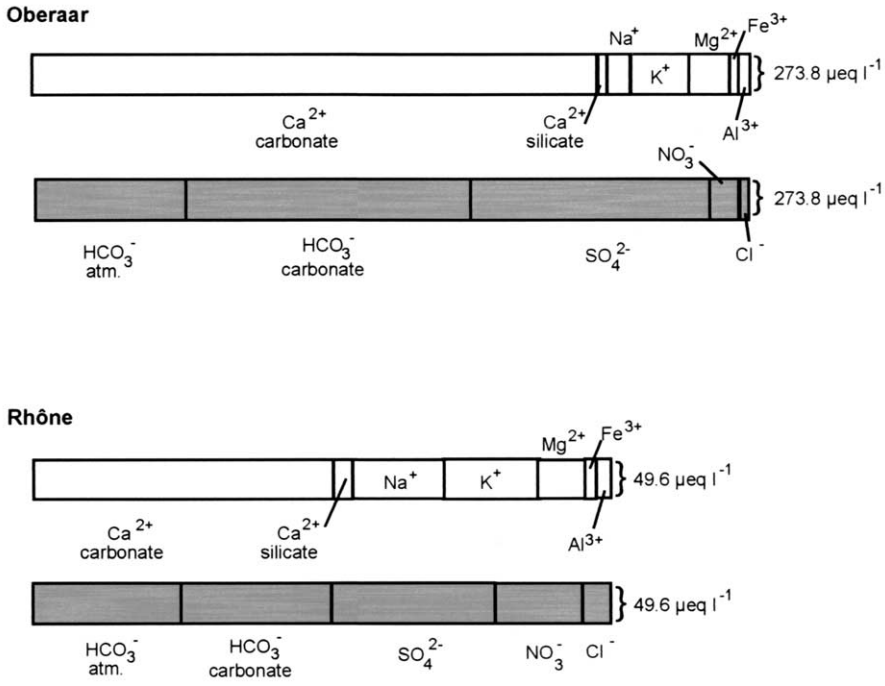

Fig. 6. The average July runoff composition.

the Oberaar catchment compared to the Rhône). The incongruent weathering of epidote may influence the Ca^{2+} flux, but again we estimate this to be of only minor importance.

Besides the unequal Ca^{2+} flux, the other salient difference between the meltwater chemistries of the Rhône and Oberaar catchments is the additional sulphide present in the Oberaar catchment, leading to the denudation of 6 times more sulphate from this catchment. (The Oberaar suspended sediment also has an elevated iron content; XRF data). The additional sulphide is probably associated with the strongly foliated gneissic zone. Raiswell (1984) demonstrated that protons derived from sulphide oxidation in the subglacial environment are important in acid hydrolysis reactions. Hence, the flux of dissolved Ca from the Oberaar catchment is in part due to the generation of 6 times as many protons by sulphide oxidation in the Oberaar's subglacial environment. But, since the meltwaters are not saturated with calcite (Table 5), the extent of weathering is still kinetically controlled, and therefore the higher available surface area of calcite in the Oberaar catchment remains an important factor. Moreover, in the Oberaar catchment atmospheric CO_2 remains a comparatively important source of protons relative to sulphide oxidation (Fig. 6). Therefore, we conclude that the higher calcium content of the Oberaar meltwaters is a cumulative result of the elevated calcite and pyrite content of the Oberaar catchment's bedrock.

4.2. Silicate Weathering

Silicate weathering is temperature dependant (Vebel, 1993; White and Blum, 1995). Re-plotting the values of White and Blum (1995) to include glacial catchments with granitoid bedrock (Fig. 7) shows that the precipitation corrected silica fluxes from presently glaciated crystalline catchments are 100 kmol km^{-2} yr^{-1} lower than those from un-glaciated crystalline catchments. Our two catchments therefore fit into the scheme proposed by Anderson et al. (1997), who used a very similar data set.

The cations derived from silicate weathering (Σ K^+, Mg^{2+}, Na^+ and Ca^{2+} from the weathering of plagioclase; $Ca_{plag,}$ see below) are 1/3 greater from the Oberaar catchment than the Rhône (Oberaar = 99; Rhône = 65 kmol km^{-2} yr^{-1}). The silicate derived cation fluxes (Σ K^+, Mg^{2+}, Na^+) from this study plot slightly below those from non-glacial catchments with similar runoff, located at similar latitudes (Fig. 8); Ca_{plag} is not included, as is not known for the published data compiled in White and Blum, 1995).

4.3. CO_2 Draw Down

Total CO_2 draw down ($CO_{2\ dd}$) in the catchments is calculated based on the precipitation corrected, chloride normalised fluxes (kmol km^{-2} yr^{-1}). We define $CO_{2\ dd}$ as the difference between the total dissolved inorganic carbon flux, that is calculated HCO_3^-, (DIC_{tot}; Rhône = 109.8; Oberaar = 468.1 kmol km^{-2} yr^{-1}) and the HCO_3^- flux released by calcite during its dissolution (DIC_{cc}).

$$CO_{2\ dd} = DIC_{tot} - DIC_{cc} = DIC - (Ca - 0.1\ Na)$$

There is a 1:1 mol/L relationship between DIC_{cc} and the Ca^{2+} flux generated by the dissolution of calcite. The annual molar flux of Ca^{2+} is 48.3 and 277.7 kmol km^{-2} yr^{-1} from the Rhône and Oberaar catchments respectively. We assume that the Ca input from the weathering of amphibole, epidote, titanite and apatite is 0. The contribution of plagioclase ($Ca_{plag,}$) to the Ca^{2+} flux is calculated stoichiometrically: Our plagioclase

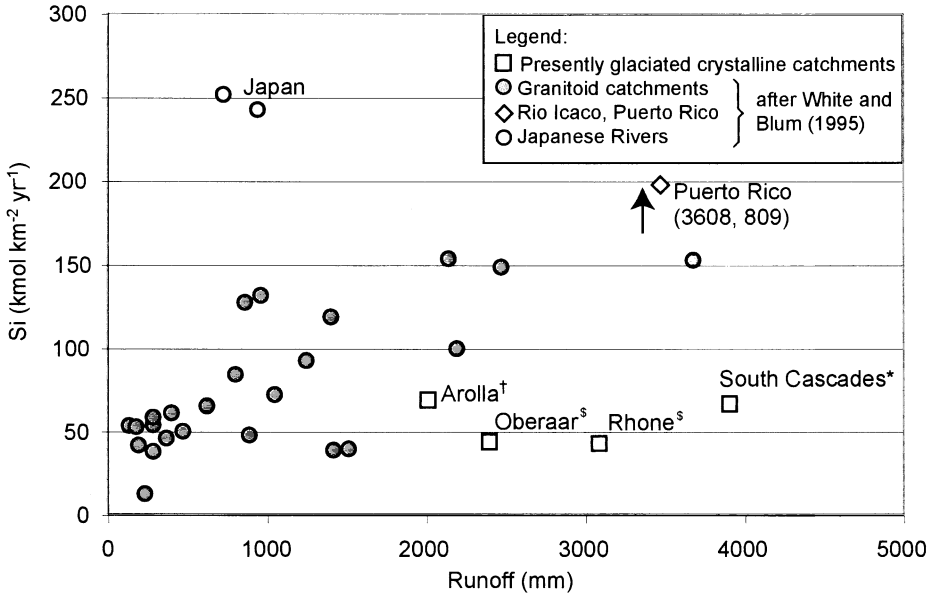

Fig. 7. Molar weathering fluxes of silica against runoff in presently glaciated and non-glaciated granitoid catchments. All fluxes are corrected for precipitation inputs: †Sharp et al. (1995), *Axtmann and Stallard (1995) and $this study, cyclical salt corrections; White and Blum (1995), volumetric correction.

feldspar is of albitic composition (Keusen et al., 1989), we therefore calculate Ca_{plag} as 10% of the Na flux (Ca_{plag}; Rhône = 2.7; Oberaar = 2.6 kmol km^{-2} yr^{-1}). Hence 25.6 and 275.2 kmol HCO_3^- km^{-2} yr^{-1} are from the calcite mineral itself.

The remainder of the HCO_3^- in solution must be derived from atmospheric CO_2. Therefore $CO_{2\ dd}$ is 64.3 kmol km^{-2} yr^{-1} in the Rhône catchment and 192.8 kmol km^{-2} yr^{-1} in the Oberaar catchment. The Oberaar value is comparable with the $CO_{2\ dd}$ calculated for the Swiss Haut Glacier d'Arolla catchment, which has a schistose bedrock geology (1989 = 166.7 kmol km^{-2} yr^{-1}; 1990 = 206.4 kmol km^{-2} yr^{-1}; Sharp et al., 1995). The long-term portion of this draw down is that amount of CO_2 that will precipitate as calcite with Ca from a silicate source. The long-term draw down is relatively small and is similar for both catchments (ca. 1.3 kmol km^{-2} yr^{-1}).

5. CONCLUSIONS

The strongly foliated gneissic zone running down the central third of the Oberaar catchment has a major impact on the physical and chemical erosion rates measured within this watershed, compared to those of the Rhône catchment, which lies on granitic and granodioritic rocks. Approximately twice as much suspended sediment was exported by the Oberaar meltwaters compared to the Rhône meltwaters during the study period (1999–2001), implying a greater erodability of the

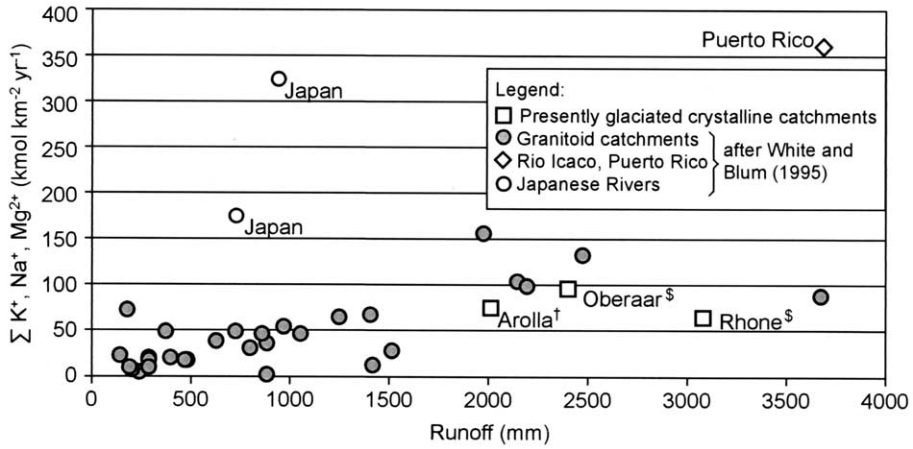

Fig. 8. Molar fluxes of cations derived from silicate weathering against runoff in presently glaciated and non-glaciated granitoid catchments. All fluxes are corrected for precipitation inputs: †Sharp et al. (1995), $this study, cyclical salt corrections; White and Blum (1995), volumetric correction.

Oberaar bedrock. This greater erodability, coupled with the larger mean calcite content of the Oberaar sediments, leads to 6–7 times more dissolved calcium being weathered from the Oberaar watershed, most of which comes from carbonate dissolution. A second reason for the greater extent of weathering in the Oberaar catchement is the availability of more protons from pyrite oxidation, as is reflected by a 6 times higher SO_4 flux. Calcite weathering is more important in this glacial catchment than in non-glaciated catchments underlain by granitoid rocks (judging by the Ca/Na molar ratios; Fig. 5). Yet both the silica and the silicate-derived-cation weathering rates we observe in our presently glaciated alpine catchments, and those published for other presently glaciated catchments, fall below the range published for non-glaciated granitoid catchments with the same runoff, Implying that silicate weathering is retarded in the subglacial environment.

Acknowledgments—We thank Daniel Arn, David Nisbet, Katharine Nisbet, and Marlen Schaller for field support and Giulio Galetti, Khaoula Hamila and Sebastian Ryser for laboratory assistance. We also thank James Drever, Suzanne Prestrud Anderson and an anonymous reviewer for their constructive comments. This study was supported by Swiss NF grants 21-53991.98 and 20-61485.00.

Associate editor: L. Kump

REFERENCES

Adatte T., Stinnesbeck W., and Keller G. (1996) Lithostratigraphic and mineralogical correlations of near K/T boundary clastic sediments in northeastern Mexico: Implications for origins and nature of deposition. In *The Cretaceous-Tertiary Event and Other Catastrophes in Earth History* (eds. G. Ryder, D. Fastovsky and S. Gartner). Geological Society of America Special Paper 307. Boulder, Colorado.

Anderson S. P., Drever J. I., and Humphery N. F. (1997) Chemical weathering in glacial environments. *Geology* **25,** 399–402.

Anderson S. P., Drever J. I., Frost C. D., and Holden P. (2000) Chemical weathering in the foreland of a retreating glacier. *Geochim. Cosmochim. Acta* **64,** 1173–1189.

Arn K. (2002) Geochemical weathering in the sub-and pro-glacial zones of two crystalline catchments in the Swiss Alps (Oberaar—Rhône glaciers). Ph. D. thesis, Univertité de Neuchâtel.

Axtmann E. V. and Stallard R. F. (1995) Chemical weathering in the South Cascade Glacier basin, comparison of sub-glacial and extra-glacial weathering. In *Geochemistry of Seasonally Snow-Covered Catchments* IAHS.**228,** 431–439. (Proceedings of a Boulder Symposium, July, 1995).

Bernath A. (1991) Zum Wasserhaushalt im Einzugsgebiet der Rhône bis Gletsch. (ed D. Grebner). *Züricher Geographische Schriften* **43,** pp 383.

Bluth G. J. S. and Kump L. R. (1994) Lithological and climatological controls of river chemistry. *Geochim. Cosmochim. Acta* **58,** 2341–2359.

Boulton G. S. (1979) Processes of glacier erosion on different substrata. *J. Glaciol.* **23,** 15–38.

Brantley S. L. and Chen Y. (1995) Chemical weathering rates of pyroxenes and amphiboles. In *Chemical weathering rates of silicate minerals* (eds. A. F. White and S. L. Brantley). *Rev. Mineral.* **31,** 119–172.

Chou L. and Wollast R. (1985) Steady state kinetics and dissolution mechanisms of albite. *Am. J. Sci.* **285,** 963–993.

Dreimanis A. and Vagners U. J. (1969) Characteristics of the composition of till derived from the basal and the englacial drift. *Geol. Soc. Am.* **6,** 1–12.

Dreimanis A., and Vagners U. J. (1971) The dependence of the composition of till upon the rule of bimodal distribution. In *Etudes sur le Quaternaire dans le Monde* **2,** pp. 787–789. Bulletin de l'Association Francaise pour l'Etude du Quaternaire 4.

Drever J. I. and Hurcomb D. R. (1986) Neutralization of atmospheric acidity by chemical weathering in an alpine drainage basin in the North Cascade Mountains. *Geology* **14,** 221–224.

Drewry D. (1986) Glacial Geological Processes. Edward Arnold, London, England.

Eyles N., Sassevilee D. R., Slatt R. M., and Rogerson R. J. (1982) Geochemical denudation rates and solute transport mechanisms in a maritime temperate glacier basin. *Can. J. Earth Sci.* **19,** 1570–1581.

Fairchild I. J., Killawee J. A., Hubbard B., and Derybrodt P. (1999) Interactions of calcareous suspended sediment with glacial meltwater: a field test of dissolution behaviour. *Chem. Geol.* **155,** 243–263.

Federal Office for Water and Geology (1994) Technischer Bericht: Manual für die Abflussmessung nach dem Salzverdünnungsverfahren.

Gibbs M. T. and Kump L. R. (1994) Global chemical erosion during the last glacial maximum and the present: Sensitivity to changes in lithology and hydrology. *Paleoceanog.* **9,** 529–543.

Gurnell A. M., Brown G. H., and Tranter M. (1994) Sampling strategy to describe the temporal hydrochemical characteristics of an alpine pro-glacial stream. *Hydrol. Proc.* **8,** 1–25.

Hallet B., Hunter L., and Bogen J. (1996) Rates of erosion and sediment evacuation by glaciers: A review of field data and their implications. *Global Planet. Change* **12,** 213–235.

Hay W. W. (1998) Detrital sediment fluxes from continents to oceans. *Chem. Geol.* **145,** 287–323.

Hosein R. (2002) Biogeochemical weathering processes in the Glacierised Rhône and Oberaar catchments, Switzerland, and the Apure catchment, Venezuela. Phd thesis, Université de Neuchâtel.

Keusen H. R., Ganguin J., Schuler P., and Buletti M. (1989) *NAGRA technischer Bericht.* 87–14.

Kübler B., Jantschik R., and Huon S. (1990) Minérologie et granulométrie des poussières éoliennes, dites "Sahariennes," du 24 avril 1989 à Neuchâtel. Leur importance pour l'environnment, les sols et les sédiments. *Bull. Soc. Neuchât. Sci. Nat.* **113,** 75–98.

Lenaz R., Landuzzi V., and Tomadin L. (1986) Apports et concentration des masses de poussières éoliennes sur le bassin oriental et occidental de al Méditerranée. *Mem. Soc. Geol. It.* **36,** 189–200.

Livingstone D. A. (1963) Chemical compositions of rivers and lakes. *U. S. Geol. Surv. Prof. Paper.* **440-G,** pp 64.

Lorrain R. D. and Souchez R. A. (1972) Sorption as a factor of in the transport of major cations by meltwaters from an Alpine glacier. *Quat. Res.* **2,** 253–256.

Ludwig W., Amiotte-Suchet P., Munhoven G., and Probst J-L. (1998) Atmospheric CO_2 consumption by continental erosion: present-day controls and implications for the last glacial maximum. *Global Planet. Change* **16,** 107–120.

Mahaney W. C. (1995) Glacial crushing, weathering and diagenetic histories of quartz grains inferred from scanning electron microscopy. In *Modern glacial environments. Processes, dynamics and sediments, Glacial Environments: Volume 1* (ed. J. Menzies), pp 621. Butterworth-Heinemann, Oxford.

Meybeck M. (1987) Global chemical weathering of surficial rocks estimated from river dissolved loads. *Am. J. Sci.* **287,** 401–428.

Mullin J. B. and Riley J. P. (1955) The colorimetric determination of silicate with special reference to sea and natural waters. *Anal. Chim. Acta* **12,** 162–176.

Nienow P., Sharp M., and Willis I. (1996) Temporal switching between englacial and sub-glacial drainage pathways: Dye tracer evidence from the Haut glacier d'Arrola, Switzerland. *Geogr. Ann.* **78,** 51–59.

Oberhänsli R. and Schenker F. (1988) Indications of Variscan nappe teconics in the Aar Massif. *Scheiz. Mineral. Petrogr. Mitteil.* **68,** 509–520.

Plummer L. N., Wigley T. M. L., and Parkhurst D. L. (1978) The kinetics of calcite dissolution in CO_2-water systems at 5–60°C and 0.0–1.0 atm CO_2. *Am. J. Sci.* **278,** 179–216.

Raiswell R. (1984) Chemical models of solute aquisition in glacial meltwaters. *J. Glaciol.* **30,** 49–57.

Schwab M., Frei C., Schär C. and Daly C. (2001) Mean annual precipitation throughout the European Alps 1971–1990. In *The Hydrological Atlas of Switzerland* (ed. Landeshydrologie, Bundesamt für Wasser und Geologie). Bundesamt für Landestopographie, Bern.

Sharp M., Tranter M., Brown G. H., and Skidmore M. (1995) Rates of chemical denudation and CO_2 draw down in a glacier-covered alpine catchment. *Geology* **23,** 61–64.

Sharp M., Parkes J., Cragg B., Fairchild I. J., Lamb H., and Tranter M. (1999) Widespread bacterial populations at glacier beds and their relationship to rock weathering and carbon cycling. *Geology* **27,** 107–110.

Slatt R. M. (1972) Geochemistry of meltwater streams from nine Alaskan glaciers. *Geol. Soc. Am. Bull.* **83,** 1125–1132.

Souchez R. A. and Lemmens M. M. (1987) Solutes: 285–303. In *Glacio-fluvial sediment transfer: An alpine perspective* (eds. A. M. Gurnell and M. J. Clark). John Wiley & Sons, New York.

Stumm W. and Morgan J. J. (1996) Aquatic Chemistry. (eds. J. L Schnoor and A. Zehnder). John Wiley & Sons.

Sugden D. E. (1978) Glacial erosion by the Laurentide ice sheet. *J. Glaciol.* **20,** 367–394.

Summerfield M. (1991) Global geomorphology. Longman, Harlow, United Kingdom.

Taylor A. and Blum J. D. (1995) Relation between soil age and silicate weathering rates from the chemical evolution of a glacial chronosequence. *Geology* **23,** 979–982.

Tranter M., Sharp M. J., Lamb H. R., Brown G. H., Hubbard B. P., and Willis I. C. (2002) Geochemical weathering at the bed of Haut Glacier d'Arolla, Switzerland—a new model. *Hydrol. Proc.* **16,** 959–993.

Vebel M. A. (1993) Temperature dependence of silicate weathering in nature: How strong a negative feedback on longterm accumulation of atmospheric CO_2 and global greenhouse warming? *Geology* **21,** 1059–1062.

West J. A., Bickle M. J., Collins R., and Brasington J. (2002) Small-catchment perspective on Himalayan weathering fluxes. *Geology* **30,** 355–358.

White A. F. and Blum A. E. (1995) Effects of climate on chemical weathering in watersheds. *Geochim. Cosmochim. Acta* **59,** 1729–1747.

White A. F., Blum A. E., Bullen T. D., Vivit D. V., Schulz M. S., and Fitzpatrick J. (1999a) The effect of temperature on experimental and natural chemical weathering rates of granitoid rocks. *Geochim. Cosmochim. Acta* **63,** 3277–3291.

White A. F., Bullen T. D., Vivit D. V., Schulz M. S., and Clow D. W. (1999b) The role of disseminated calcite in the chemical weathering of granitoid rocks. *Geochim. Cosmochim. Acta* **63,** 1939–1953.

White A. F. and Brantley S. L. (1995) Chemical weathering rates of silicate minerals: An overview. In *Chemical weathering of Silicate Minerals* (eds. A. F. White and S. L. Brantley) pp 58. Mineralogical Society of America. Washington DC.